

Optimal incident energies for production of neutron-deficient actinide nuclei in the reaction $^{58}\text{Ni} + ^{238}\text{U}$

Long Zhu,^{1,*} Jun Su,¹ and Pei-Wei Wen²

¹*Sino-French Institute of Nuclear Engineering and Technology, Sun Yat-sen University, Zhuhai 519082, China*

²*The Key Laboratory of Beam Technology and Material Modification of Ministry of Education, College of Nuclear Science and Technology, Beijing Normal University, Beijing 100875, China*

(Received 24 February 2017; published 13 April 2017)

The reaction $^{58}\text{Ni} + ^{238}\text{U}$ is investigated within the framework of dinuclear system model. The incident energy effects on production cross sections of actinide nuclei are studied. It is found that the optimal incident energies for producing neutron-deficient isotopes are larger than those for production of neutron-rich ones, and for producing neutron-deficient isotopes the optimal incident energies strongly depend on neutron richness of objective products.

DOI: [10.1103/PhysRevC.95.044608](https://doi.org/10.1103/PhysRevC.95.044608)

I. INTRODUCTION

Due to the “curvature” of the stability line and lack of sufficiently neutron-rich projectile-target combinations, it is quite hard to produce new neutron-rich isotopes of heavy and superheavy nuclei through fusion reactions. Alternatively, the multinucleon transfer process, as has been pointed out, can be used for production of exotic nuclei.

Many experiments about transfer reactions had been performed in the 1970s up to the 1990s [1–5]. Several isotopes of Fm and Md have been synthesized in the transfer reaction $^{238}\text{U} + ^{248}\text{Cm}$. It is noticed that the cross section of 0.1 μb has been reached. However, with increasing charge number of survival products the production cross section decreases strongly. Also, it is difficult to perform these experiments because of the high radiation that might destroy the detectors and problems with separating and detecting the heavy reaction products. To better understand mechanisms of heavy elements synthesis in the r process, the production of neutron-rich nuclei along $N = 126$ through multinucleon transfer process has also been studied [6–10]. These nuclei are presently produced in fragmentation reactions at relativistic energies [11]. In Ref. [8], in comparison to fragmentation reactions, the huge advantages of using the multinucleon transfer process for the production of very neutron-rich nuclei with $N = 126$ were noticed. It is also found that the advantages become more and more striking when the atomic number is lower. Multinucleon transfer process is also appropriate for producing neutron-deficient isotopes with proton numbers reaching far beyond uranium [12]. Five new neutron-deficient isotopes ^{216}U , ^{219}Np , ^{223}Am , ^{229}Am , and ^{233}Bk were observed in the reaction $^{48}\text{Ca} + ^{248}\text{Cm}$ [12].

The fundamental mechanisms of the multinucleon transfer process were investigated many years ago [13,14]. Recently, the low energy dissipative collisions of heavy ions were studied by Zagrebaev and Greiner [15–17]. It is noticed that shell

effects may significantly enhance the yield of neutron-rich heavy nuclei for appropriate projectile-target combinations [17,18]. The semiclassical model GRAZING [19], time-dependent Hartree-Fock approach (TDHF) [20–22], microscopic constrained molecular dynamics model (CoMD) [23–25], deep-inelastic transfer (DIT) model [24–26], and improved quantum molecular dynamics model (ImQMD) [27–29] are also used to investigate the mechanisms of deep inelastic collisions of heavy ions. The dinuclear system (DNS) model, which can treat the charge, mass, angular momentum, and kinetic energy dissipation during heavy ion collisions, has been successfully used in investigating the multinucleon transfer reactions [30–35]. The production of neutron-rich isotopes around $N = 126$ shell closure in radioactive beam induced transfer reactions are investigated [33]. It is found that, based on the target ^{208}Pb , the radioactive beam ^{144}Xe shows great advantages for producing neutron-rich nuclei with $N = 126$ in comparison to the stable beam ^{136}Xe and the advantages get more obvious for producing nuclei with less charge number.

The production cross sections of exotic heavy nuclei through transfer reactions strongly depend on the projectile-target combination and the incident energy [36]. In Ref. [16], it was pointed out that optimal beam energy for production of neutron-rich nuclei in transfer reactions is about 20–30 MeV higher than the corresponding Coulomb barrier in the entrance channel. For production of neutron-deficient heavy nuclei the optimal incident energy (OPE) should be quite different.

In this work, the transfer reaction $^{58}\text{Ni} + ^{238}\text{U}$ is investigated within the framework of the DNS model. The influences of incident energy on production cross sections of neutron-rich and neutron-deficient actinide nuclei are studied. The OPEs for producing some unknown actinide isotopes located at the neutron-deficient side with $Z = 93–97$ in the reaction $^{58}\text{Ni} + ^{238}\text{U}$ are predicted.

The article is organized as follows. In Sec. II, we describe the theoretical framework in detail. The results and discussion are presented in Sec. III. Finally, we summarize the main results in Sec. IV.

* Corresponding author: zhulong@mail.sysu.edu.cn

II. THEORETICAL FRAMEWORK

The production cross sections of the final products in transfer reactions can be written as

$$\sigma_{\text{ER}}(Z_1, N_1 - x) = \frac{\pi \hbar^2}{2\mu E_{\text{c.m.}}} \sum_{J=0}^{J_{\text{max}}} (2J+1) T_{\text{trans}}(J) \times P(Z_1, N_1, t = \tau_{\text{int}}) W_{\text{sur}}(xn), \quad (1)$$

where the interaction time τ_{int} , which is determined by deflection function method [37], is strongly affected by interaction potential at the contact configuration, incident energy, and entrance angular momentum J . Because of the incident energy dissipation, the primary fragments are excited. Therefore, the survival probability $W_{\text{sur}}(xn)$ is considered. x is the number of neutrons evaporated from the excited primary fragments.

T_{trans} is the Coulomb barrier transmission probability, which can be calculated as

$$T_{\text{trans}}(E_{\text{c.m.}}, J) = \frac{1}{1 + \exp\left\{-\frac{2\pi}{\hbar\omega(J)} \left[E_{\text{c.m.}} - B - \frac{\hbar^2}{2\mu R_{\text{B}}^2(J)}\right]\right\}}. \quad (2)$$

Here, $E_{\text{c.m.}}$ is the incident energy at the center of mass frame. $\hbar\omega(J)$ is the width of the parabolic barrier, $R_{\text{B}}(J)$ defines a position of the barrier. B is the height of Coulomb barrier. For multinucleon transfer reactions in collisions of heavy nuclei with no potential pocket and the incident energies are above the interaction potentials at the contact configurations (there are no ordinary barriers: the potential energies of these nuclei are everywhere repulsive), it is reasonable to take the value of T_{trans} as 1.

$P(Z_1, N_1, t)$ is the distribution probability for fragment with proton number Z_1 and neutron number N_1 at time t , which can be calculated by solving the master equation:

$$\begin{aligned} \frac{dP(Z_1, N_1, t)}{dt} = & \sum_{Z'_1} W_{Z_1, N_1; Z'_1, N_1}(t) [d_{Z_1, N_1} P(Z'_1, N_1, t) \\ & - d_{Z'_1, N_1} P(Z_1, N_1, t)] \\ & + \sum_{N'_1} W_{Z_1, N_1; Z_1, N'_1}(t) [d_{Z_1, N_1} P(Z_1, N'_1, t) \\ & - d_{Z_1, N'_1} P(Z_1, N_1, t)] \\ & - [\Lambda_{\text{qf}}(\Theta(t))] P(Z_1, N_1, t). \end{aligned} \quad (3)$$

Here, $W_{Z_1, N_1; Z'_1, N_1}$ ($W_{Z_1, N_1; Z_1, N'_1}$) denotes the mean transition probability from the channel (Z_1, N_1) to (Z'_1, N_1) [or (Z_1, N_1) to (Z_1, N'_1)], and d_{Z_1, N_1} is the microscopic dimension corresponding to the macroscopic state (Z_1, N_1) . In the DNS model, we consider the process of only one nucleon transfer. The sum is taken over all possible proton and neutron numbers that fragment 1 may take. Λ_{qf} is the quasifission (QF) rate, which describes the evolution of DNS system along relative distance R , which can be treated with the one-dimensional

Kramers rate [38]:

$$\Lambda_{\text{qf}}(\Theta(t)) = \frac{\omega}{2\pi\omega^{B_{\text{qf}}}} \left[\sqrt{\left(\frac{\Gamma}{2\hbar}\right)^2 + (\omega^{B_{\text{qf}}})^2} - \frac{\Gamma}{2\hbar} \right] \times \exp\left[-\frac{B_{\text{qf}}(Z_1, N_1)}{\Theta(t)}\right]. \quad (4)$$

The QF rate exponentially depends on the QF barrier B_{qf} . The local temperature $\Theta(t)$ is calculated by using Fermi-gas expression $\Theta = \sqrt{\varepsilon^*/a}$ with the local excitation energy ε^* and the level-density parameter $a = A/12 \text{ MeV}^{-1}$. The frequency $\omega^{B_{\text{qf}}}$ of the inverted harmonic oscillator approximates the potential V in R at the top of the quasifission barrier, and ω is the frequency of the harmonic oscillator approximating the potential in R around the bottom of the pocket. The Γ determines the friction coefficients. Here, $\Gamma = 2.8 \text{ MeV}$, $\hbar\omega^{B_{\text{qf}}} = 2.0 \text{ MeV}$, and $\hbar\omega = 3.0 \text{ MeV}$. The local excitation energy is defined as

$$\varepsilon^* = E_{\text{diss}} - [U(Z_1, N_1) - U(Z_{\text{p}}, N_{\text{p}})]. \quad (5)$$

Here, E_{diss} is the energy dissipated into the initial composite system from the incident energy, which depends on entrance angular momentum J . During the diffusion process, the relative kinetic energy will dissipate into the DNS system. The potential energy surface (PES) in collisions of actinide nuclei can be written as

$$U(Z_1, N_1, R_{\text{cont}}) = B(Z_1, N_1) + B(Z_2, N_2) + V(Z_1, N_1, R_{\text{cont}}). \quad (6)$$

Here, $B(Z_i, N_i)$ ($i = 1, 2$) is the ground state binding energy of the fragment i . The effective nucleus-nucleus interaction potential $V(Z_1, N_1, R_{\text{cont}})$ is calculated at the contact point of two fragments and can be written as

$$V(Z_1, N_1, R_{\text{cont}}) = V_{\text{N}}(Z_1, N_1, R_{\text{cont}}) + V_{\text{C}}(Z_1, N_1, R_{\text{cont}}), \quad (7)$$

where $R_{\text{cont}} = R_1(1 + \beta_1 Y_{20}(\theta_1)) + R_2(1 + \beta_2 Y_{20}(\theta_2)) + 0.7 \text{ fm}$. Here, $R_{1,2} = 1.16 A_{1,2}^{1/3}$. $\beta_{1,2}$ is the quadrupole deformation parameter of the fragments and is taken from Ref. [39]. θ_i is the angle between the symmetry axis of the i th nucleus and the collision axis. We take θ_i equals 0 for tip-tip collisions. Figure 1 shows the PES as a function of charge asymmetry for the reaction $^{58}\text{Ni} + ^{238}\text{U}$. If the excitation energy of DNS is not high enough, the DNS may easily decay into two fragments after multinucleon transfer from a heavy fragment into a light one.

The nuclear potential can be written as [40]

$$\begin{aligned} V_{\text{N}}(r, \theta) = & C_0 \left\{ \frac{F_{\text{in}} - F_{\text{ex}}}{\rho_0} \left[\int \rho_1^2(\mathbf{r}) \rho_2(\mathbf{r} - \mathbf{R}) d\mathbf{r} \right. \right. \\ & + \left. \int \rho_1(\mathbf{r}) \rho_2^2(\mathbf{r} - \mathbf{R}) d\mathbf{r} \right] \\ & \left. + F_{\text{ex}} \int \rho_1(\mathbf{r}) \rho_2(\mathbf{r} - \mathbf{R}) d\mathbf{r} \right\} \end{aligned} \quad (8)$$

with

$$F_{\text{in,ex}} = f_{\text{in,ex}} + f'_{\text{in,ex}} \frac{N_1 - Z_1}{A_1} \frac{N_2 - Z_2}{A_2}. \quad (9)$$

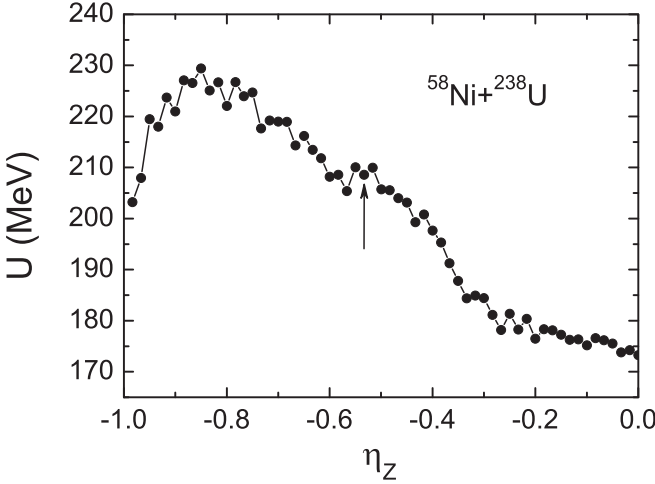


FIG. 1. The PES for the reaction $^{58}\text{Ni} + ^{238}\text{U}$ as a function of charge asymmetry [$\eta_Z = (Z_1 - Z_2)/(Z_1 + Z_2)$]. The arrow indicates the entrance channel.

Here, $C_0 = 300$ MeV, $f_{\text{in}} = 0.09$, $f_{\text{ex}} = -2.59$, $f'_{\text{in}} = 0.42$, and $f'_{\text{ex}} = 0.54$. Z_1 (N_1) and Z_2 (N_2) are the charge (neutron) number of light and heavy fragments, respectively. The density distributions of two nuclei are expressed as Woods-Saxon distribution as

$$\rho_1(\mathbf{r}) = \frac{\rho_0}{1 + \exp[(\mathbf{r} - \mathfrak{R}_1(\theta_1))/a_1]} \quad (10)$$

and

$$\rho_2(\mathbf{r}-\mathbf{R}) = \frac{\rho_0}{1 + \exp[(|\mathbf{r}-\mathbf{R}| - \mathfrak{R}_2(\theta_2))/a_2]} \quad (11)$$

Here, $\rho_0 = 0.16$ fm $^{-3}$. $\mathfrak{R}_i = R_i[1 + \beta_i Y_{20}(\theta_i)]$ is the surface radii of the collision nuclei. β_i and R_i are quadrupole deformation parameter and the spherical radius of the i th nucleus, respectively. The diffuseness parameter equals 0.56–0.58 fm, which depends on the mass number. \mathbf{R} is the distance between the centers of two fragments.

The Coulomb potential is taken as the form in Ref. [41]

$$V_C(r, \theta_i) = \frac{Z_1 Z_2 e^2}{r} + \left(\frac{9}{20\pi}\right)^{1/2} \left(\frac{Z_1 Z_2 e^2}{r^3}\right) \times \sum_{i=1}^2 R_i^2 \beta_2^{(i)} P_2(\cos\theta_i) + \left(\frac{3}{7\pi}\right) \left(\frac{Z_1 Z_2 e^2}{r^3}\right) \sum_{i=1}^2 R_i^2 [\beta_2^{(i)} P_2(\cos\theta_i)]^2. \quad (12)$$

The survival probability of the excited fragments in the process of its cooling by means of neutron evaporation in the competition with fission and emission of light charged particles ($C \rightarrow B + xn$) is estimated usually within the statistical model of atomic nuclei and can be written as

$$W_{\text{sur}}(E^*, xn) = P(E^*, xn) \times \prod_{i=1}^{xn} \left[\frac{\Gamma_n(E_i^*)}{\Gamma_{\text{tot}}(E_i^*)} \right], \quad (13)$$

where E^* is the excitation energy of one primary fragment. E_i^* is the excitation energy before evaporation of the i th neutron, which can be calculated from the equation $E_{i+1}^* = E_i^* - B_n^i - 2T_i$. B_i is the separation energy of i th neutron. T_i is nuclear temperature before evaporating the i th neutron and obtained from $E_i^* = aT_i^2 - T_i$. The realization probability $P(E^*, xn)$ can be seen in Refs. [42,43]. $\Gamma_{\text{tot}} = \Gamma_n + \Gamma_f + \Gamma_p + \Gamma_\alpha + \Gamma_d$. The partial decay widths of the compound nucleus for the evaporation of the light particle $a = (n, p, \alpha, d)$ can be estimated using the Weisskopf-Ewing theory [44,45]

$$\Gamma_{C \rightarrow B+a}(E_i^*, J) = \frac{2s_a + 1}{2\pi\rho_C(E_i^*, J)} \frac{2m_a R^2}{\hbar^2} \int_0^{E_i^* - B_a^i - \delta} \times \varepsilon T_a(\varepsilon) \rho_B(E_i^* - B_a^i - \varepsilon, J) d\varepsilon. \quad (14)$$

Here, s_a , R , and m_a are the spin of evaporated light particle, radius of the daughter nucleus B , and mass of light particle. $T_a = \{1 + \exp[-\frac{2\pi}{\hbar\omega_B}(\varepsilon - V_a)]\}^{-1}$ is the penetration probability of the Coulomb barrier. $R_a = 1.16 \times (A_B^{1/3} + A_a^{1/3})$.

On the other hand, the fission decay width is usually calculated within the Bohr-Wheeler (BW) transition-state method [46]:

$$\Gamma_f(E_i^*, J) = \frac{1}{2\pi\rho_C(E_i^*, J)} \int_0^{E_i^* - B_f^i} \times \frac{\rho_C(E_i^* - B_f^i - \delta)}{1 + \exp[2\pi(\varepsilon + B_f^i - E_i^*)/\hbar\omega]} d\varepsilon. \quad (15)$$

In this work, the fission barrier is obtained by $B_f(E^*) = B_f^{\text{mac}} - \Delta E_{\text{shell}} e^{-E^*/E_d}$. ΔE_{shell} is shell correction to the nucleus ground state. The macroscopic part of the fission barrier B_f^{mac} is calculated using the liquid drop model. The damping parameter $E_d = 18.5$ MeV.

III. RESULTS AND DISCUSSION

Figure 2(a) shows the cross sections for formation of Neptunium isotopes ($Z = 93$) in collisions $^{58}\text{Ni} + ^{238}\text{U}$ at different incident energies. It is clearly shown that the yields of primary fragments increase strongly with the increasing incident energy. However, due to incident energy dissipation, the increasing incident energy increases the excitation energy of these fragments and thus decreases their survival probability. It is noticed that the yield distribution of final fragments increases at first and then decreases with the increasing incident energy. This is mainly due to the competition between incident energy effects of primary fragments yields and their survival probabilities. The production cross sections of $E_{\text{c.m.}} = 380$ MeV, in comparison with those of $E_{\text{c.m.}} = 290$ MeV, are strongly depressed at the region with $A > 225$. However, for production of very neutron-deficient isotopes ($A < 220$), the cross sections of $E_{\text{c.m.}} = 380$ MeV are larger. This is because more neutrons can be evaporated in competition with fission for higher incident energy and enhance the yields of neutron-deficient isotopes. Hence, the OPEs for producing neutron-deficient isotopes should be larger than those for neutron-rich isotopes.

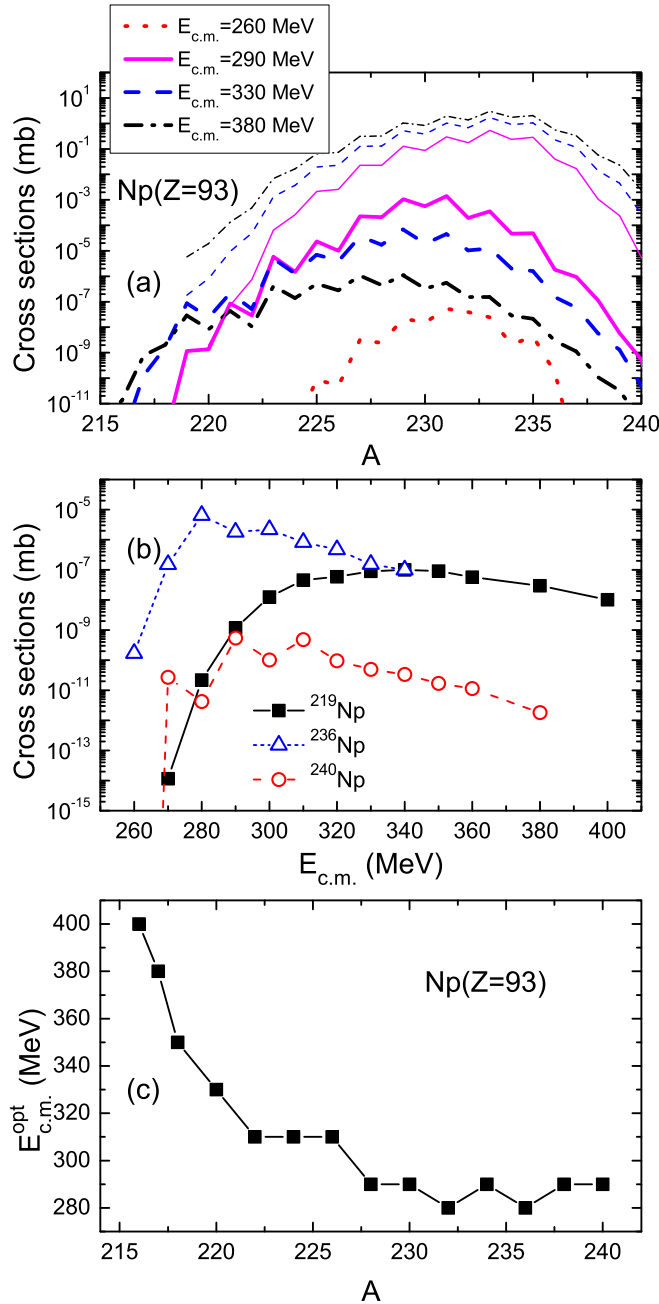


FIG. 2. (a) Cross sections for formation of neptunium isotopes ($Z = 93$) in collisions $^{58}\text{Ni} + ^{238}\text{U}$ at different incident energies. The thin and thick lines denote distribution of primary and surviving fragments, respectively. (b) Cross sections as a function of beam energy for production of neutron-deficient nucleus ^{219}Np and neutron-rich nuclei $^{236,240}\text{Np}$ in the reaction $^{58}\text{Ni} + ^{238}\text{U}$. (c) The OPEs for producing different neptunium isotopes ($Z = 93$) in the reaction $^{58}\text{Ni} + ^{238}\text{U}$. The energy is discretized by 10 MeV.

In order to see the difference of OPEs between production of neutron-deficient and neutron-rich nuclei, we show in Fig. 2(b) the incident energy dependence of cross sections for production of ^{219}Np and $^{236,240}\text{Np}$ nuclei. We notice that for these nuclei the cross sections increase first and then decrease with the increasing incident energy. It can be seen clearly that

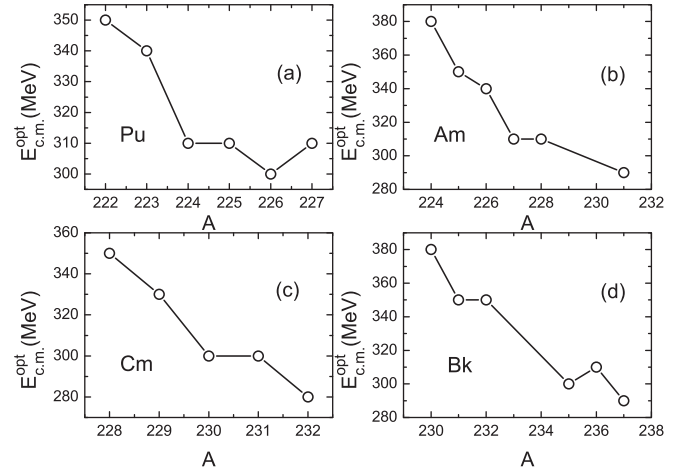


FIG. 3. The predicted OPEs for producing unknown isotopes located at the neutron-deficient side with $Z = 94-97$ in the transfer reaction $^{58}\text{Ni} + ^{238}\text{U}$. The energy is discretized by 10 MeV. The lines are used to guide the eye.

the incident energy for maximal production cross section of ^{240}Np is 290 MeV. However, the OPE for producing ^{219}Np isotope is 340 MeV, which is much larger than those for producing $^{236,240}\text{Np}$.

In Fig. 2(c), the OPEs $E_{c.m.}^{opt}$ for producing different neptunium isotopes in the reaction $^{58}\text{Ni} + ^{238}\text{U}$ are shown. For production of ^{216}Np , the calculated OPE is 400 MeV. We can see that the OPE increases strongly with the decreasing mass number for $A \leq 222$, and the curve is almost flat in neutron-rich region. The Coulomb barrier of the reaction $^{58}\text{Ni} + ^{238}\text{U}$ is 249 MeV. For production of neutron-rich isotopes the OPEs are close to 1.1 times the Coulomb barrier. However, for producing ^{216}Np , the OPE is almost 1.6 times the Coulomb barrier. With the increasing incident energy, the excitation energies of primary fragments increase. Hence, more neutrons can be evaporated, which will contribute to the yields of more neutron-deficient isotopes. However, this kind of contribution to yields of neutron-rich isotopes is slight. Therefore, the OPEs are close in neutron-rich region.

In order to produce more unknown neutron-deficient actinide isotopes, we predict OPEs for producing unknown isotopes located at the neutron-deficient side with $Z = 94-97$ in the transfer reaction $^{58}\text{Ni} + ^{238}\text{U}$ and show in Fig. 3. The trend can be seen that for each element the OPE increases strongly with decreasing mass number. For producing unknown nuclei ^{222}Pu , ^{225}Am , ^{228}Cm , and ^{231}Bk in the reaction $^{58}\text{Ni} + ^{238}\text{U}$, the OPE is close 1.4 times the Coulomb barrier.

IV. CONCLUSIONS

Within the framework of DNS model, the transfer reaction $^{58}\text{Ni} + ^{238}\text{U}$ for production of actinide nuclei is investigated. The incident energy dependence of production cross sections of neutron-rich and neutron-deficient isotopes is studied. It is found that the OPEs for producing neutron-deficient isotopes are larger than those for production of neutron-rich ones. Also,

for producing neutron-deficient isotopes the optimal incident energies strongly depend on neutron richness of objective products. For producing neutron-rich isotopes, the OPEs are very close. We also predict the OPEs for producing some unknown neutron-deficient actinide nuclei with $Z = 94-97$ in the reaction $^{58}\text{Ni} + ^{238}\text{U}$. It is found that for producing unknown neutron-deficient nuclei ^{222}Pu , ^{225}Am , ^{228}Cm , and ^{231}Bk in the reaction $^{58}\text{Ni} + ^{238}\text{U}$, the OPE is close 1.4 times the Coulomb barrier.

ACKNOWLEDGMENTS

This work was supported by the National Natural Science Foundation of China under Grant No. 11605296; the Natural Science Foundation of Guangdong Province, China (Grant No. 2016A030310208); the National Natural Science Foundation of China under Grant No. 11405278; the Fundamental Research Funds for the Central Universities under Grant No. 151gpy30.

-
- [1] K. D. Hildenbrand, H. Freiesleben, F. Pühlhofer, W. F. W. Schneider, R. Bock, D. v. Harrach, and H. J. Specht, *Phys. Rev. Lett.* **39**, 1065 (1977).
- [2] M. Schadel, J. V. Kratz, H. Ahrens, W. Bruchle, G. Franz, H. Gaggeler, I. Warnecke, G. Wirth, G. Herrmann, N. Trautmann, and M. Weis, *Phys. Rev. Lett.* **41**, 469 (1978).
- [3] H. Freiesleben, K. D. Hildenbrand, F. Pühlhofer, W. F. W. Schneider, R. Bock, D. V. Harrach, and H. J. Specht, *Z. Phys. A* **292**, 171 (1979).
- [4] M. Schadel, W. Bruchle, H. Gaggeler, J. V. Kratz, K. Summerer, G. Wirth, G. Herrmann, R. Stakemann, G. Tittel, N. Trautmann, J. M. Nitschke, E. K. Hulet, R. W. Lougheed, R. L. Hahn, and R. L. Ferguson, *Phys. Rev. Lett.* **48**, 852 (1982).
- [5] R. B. Welch, K. J. Moody, K. E. Gregorich, D. Lee, and G. T. Seaborg, *Phys. Rev. C* **35**, 204 (1987).
- [6] E. M. Kozulin, E. Vardaci, G. N. Knyazheva, A. A. Bogachev, S. N. Dmitriev, I. M. Itkis, M. G. Itkis, A. G. Knyazev, T. A. Loktev, K. V. Novikov, E. A. Razinkov, O. V. Rudakov, S. V. Smirnov, W. Trzaska, and V. I. Zagrebaev, *Phys. Rev. C* **86**, 044611 (2012).
- [7] J. S. Barrett, W. Loveland *et al.*, *Phys. Rev. C* **91**, 064615 (2015).
- [8] Y. X. Watanabe, Y. H. Kim *et al.*, *Phys. Rev. Lett.* **115**, 172503 (2015).
- [9] V. I. Zagrebaev and W. Greiner, *Phys. Rev. C* **83**, 044618 (2011).
- [10] V. Zagrebaev and W. Greiner, *Phys. Rev. Lett.* **101**, 122701 (2008).
- [11] J. Kurcewicz, F. Farinon, H. Geissel *et al.*, *Phys. Lett. B* **717**, 371 (2012).
- [12] H. M. Devaraja, S. Heinz, O. Beliuskina, V. Comas *et al.*, *Phys. Lett. B* **748**, 199 (2015).
- [13] W. Cassing and W. Nörenberg, *Nucl. Phys. A* **401**, 467 (1983).
- [14] W. Nörenberg, *Phys. Lett. B* **52**, 289 (1974).
- [15] V. I. Zagrebaev, Yu. Ts. Oganessian, M. G. Itkis, and W. Greiner, *Phys. Rev. C* **73**, 031602(R) (2006).
- [16] V. I. Zagrebaev and W. Greiner, *Phys. Rev. C* **87**, 034608 (2013).
- [17] V. I. Zagrebaev and W. Greiner, *J. Phys. G: Nucl. Part. Phys.* **34**, 2265 (2007).
- [18] E. M. Kozulin, G. N. Knyazheva, S. N. Dmitriev, I. M. Itkis, M. G. Itkis, T. A. Loktev, K. V. Novikov, A. N. Baranov, W. H. Trzaska, E. Vardaci, S. Heinz, O. Beliuskina, and S. V. Khlebnikov, *Phys. Rev. C* **89**, 014614 (2014).
- [19] R. Yanez and W. Loveland, *Phys. Rev. C* **91**, 044608 (2015).
- [20] C. Golabek and C. Simenel, *Phys. Rev. Lett.* **103**, 042701 (2009).
- [21] D. J. Kedziora and C. Simenel, *Phys. Rev. C* **81**, 044613 (2010).
- [22] K. Sekizawa and K. Yabana, *Phys. Rev. C* **88**, 014614 (2013).
- [23] G. A. Souliotis, *J. Phys. Conf. Series* **205**, 012019 (2010).
- [24] N. Vonta, G. A. Souliotis *et al.*, *Phys. Rev. C* **94**, 064611 (2016).
- [25] P. N. Fountas, G. A. Souliotis, M. Veselsky, and A. Bonasera, *Phys. Rev. C* **90**, 064613 (2014).
- [26] L. Tassan-Got and C. Stefan, *Nucl. Phys. A* **524**, 121 (1991).
- [27] K. Zhao, Z. Li, Y. Zhang, N. Wang, Q. Li, C. Shen, Y. Wang, and X. Wu, *Phys. Rev. C* **94**, 024601 (2016).
- [28] N. Wang and L. Guo, *Phys. Lett. B* **760**, 236 (2016).
- [29] C. Li, F. Zhang, J. Li, L. Zhu, J. Tian, N. Wang, and F. S. Zhang, *Phys. Rev. C* **93**, 014618 (2016).
- [30] L. Zhu, Z. Q. Feng, and F. S. Zhang, *J. Phys. G: Nucl. Part. Phys.* **42**, 085102 (2015).
- [31] L. Zhu, J. Su, W. J. Xie, and F. S. Zhang, *Phys. Rev. C* **94**, 054606 (2016).
- [32] Z. Q. Feng, G. M. Jin, and J. Q. Li, *Phys. Rev. C* **80**, 067601 (2009).
- [33] L. Zhu, J. Su, W. J. Xie, and F. S. Zhang, *Phys. Lett. B* **767**, 437 (2017).
- [34] G. G. Adamian, N. V. Antonenko, V. V. Sargsyan, and W. Scheid, *Phys. Rev. C* **81**, 024604 (2010).
- [35] G. G. Adamian, N. V. Antonenko, and A. S. Zubov, *Phys. Rev. C* **71**, 034603 (2005).
- [36] J. V. Kratz, W. Loveland, and K. J. Moody, *Nucl. Phys. A* **944**, 117 (2015).
- [37] J. Q. Li and G. Wolschin, *Phys. Rev. C* **27**, 590 (1983).
- [38] G. G. Adamian, N. V. Antonenko, and W. Scheid, *Phys. Rev. C* **68**, 034601 (2003).
- [39] P. Möller, J. R. Nix, W. D. Myers, and W. J. Swiatecki, *At. Data Nucl. Data Tables* **59**, 185 (1995).
- [40] L. Zhu, J. Su, and F. S. Zhang, *Phys. Rev. C* **93**, 064610 (2016).
- [41] C. Y. Wong, *Phys. Rev. Lett.* **31**, 766 (1973).
- [42] J. D. Jackson, *Can. J. Phys.* **34**, 767 (1956).
- [43] Z. Q. Feng, G. M. Jin, F. Fu, and J. Q. Li, *Nucl. Phys. A* **771**, 50 (2006).
- [44] V. F. Weisskopf, *Phys. Rev.* **52**, 295 (1937).
- [45] V. F. Weisskopf and D. H. Ewing, *Phys. Rev.* **57**, 472 (1940).
- [46] N. Bohr and J. A. Wheeler, *Phys. Rev.* **56**, 426 (1939).